Journal of
NANOSTRUCTURES
JNS
NANOSTRUCTURES
JNS.kashanu.ac.ir

Nonlocal Vibration Behavior of a Viscoelastic SLGS Embedded on Visco-Pasternak Foundation Under Magnetic Field

A. Ghorbanpour-Arani[a,b,*], M. Shokravi[a]

[a]Faculty of Mechanical Engineering, [b]Institute of Nanoscience & Nanotechnology, University of Kashan,Kashan, I.R.Iran.

Article history:
Received 24/10/2013
Accepted 3/12/2013
Published online 1/3/2014

Keywords:
Nonlocal vibration
Surface effect
Magnetic field
Visco-Pasternak foundation
Viscoelastic SLGS

**Corresponding author:*
E-mail address*:*
aghorban@kashanu.ac.ir
Phone: +98 3615912450
Fax: +98 3615912424

Abstract

This paper is concerned with the surface and small scale effects on transverse vibration of a viscoelastic single-layered graphene sheet (SLGS) subjected to an in-plane magnetic field. The SLGS is surrounded by an elastic medium which is simulated as Visco-Pasternak foundation. In order to investigate the small scale effects, the nonlocal elasticity theory is employed due to its simplicity and accuracy. The effect of structural damping of SLGS is taken into account based on Kelvin's model on elastic materials. An analytical method is used to obtain the natural frequency of the system. A detailed parametric study is conducted to elucidate the effects of the surface layers, nonlocal parameter, magnetic field, Visco-Pasternak elastic medium, viscoelastic structural damping coefficient and aspect ratio of graphene sheet. The findings indicate that enhancing the magnetic field and the density of surface layers leads to an increase in the natural frequency of SLGS.

1. Introduction

It is commonly believed in the scientific community that nanotechnology will spark a series of industrial revolutions in the following decades. In recent years, nano-structur al carbon materials have received considerable interest by scientific communities due to their superior properties. Among carbon based nanomaterials, SLGSs have attracted many researchers for their strong mechanical strength (Young's modulus=1.0 TPa), large thermal conductivity (thermal conductivity=3000 W/km), excellent electric conductivity (electric conductivity up to 6000 S/cm), high surface area and unusual optical properties. [1,2]. These superior properties have made SLGSs promising candidates in many applications such as nanosensors, nanoelectronics, nanocomposites, batteries, nanooscillators, nanoactuators, nanoresonators, nano-optomechanical systems, supercapicitores, fuel

cells, solar cells, and hydrogen storage [3,4]. The application of the SLGS like mass sensor was investigated by Sakhaee-Pour et al. [5]. Recently, the vibration characteristics of the graphene sheets (GSs) have attracted attention of many researchers for their superior vibrational behaviors. For instance Ansari et al. [6] studied the vibrational behaviors of SLGS based on the first order shear deformation theory (FSDT) and solved the differential equations by means of generalized differential quadrature method (GDQM) for various boundary conditions. And Pradhan and Kumar [7] investigated vibration analysis of embedded orthotropic GSs.

The classical (local) theory assumes that the stress at a defined point depends uniquely on the strain at the same point. Hence, it is a scale independent theory and cannot handle size-dependent manner. There are theories that show the size-dependent behavior such as nonlocal, couple stress, modified couple stress and strain gradient. Many studies have been carried out on the basis of the nonlocal elasticity theory which was initiated in the papers byEringen [8]. He regarded the stress state at a given point as a function of the strain states of all points in the body. Pradhan and Murmu [9] studied the small scale effect on the buckling of embedded SLGS based on nonlocal plate theory. They found that the buckling loads of SLGS are strongly dependent on the small scale coefficients. In another attempt, small-scale effects on the free in-plane vibration of nanoplates were investigated by Murmu and Pradhan [10], who employed nonlocal continuum mechanics. They showed that the nonlocal effects are quite significant in in-plane vibration studies and cannot be neglected in the continuum model of graphene sheets. Nonlocal plate model for nonlinear vibration of SLGSs in thermal environment was presented by Shena et al. [11]. Their results indicated that with properly selected small scale parameters and material properties, the nonlocal plate model can provide a remarkably accurate prediction of the graphene sheet behavior under nonlinear vibration in thermal environments.

The surface-to-bulk energy ratio increasesin nanoscale problems.Therefore, surface effects must be taken into account while they can be disregarded in macroscopic structural problems. Higher-order surface stress effects on buckling of nanowires under uniaxial compression were studied by Chiu and Chen [12]. They described the mathematical framework of surface/interface stresses by generalized Young-Laplace equations based on the membrane theory. Using a generalized form of Kirchhoff plate model, Assadi [13] presented an analytical method to study the size-dependent forced vibration of rectangular nanoplates under general external loadings. The effect of surface-stress on the concentration of stress at nanoscale surface flaws was investigated by Gill [14]. And Lu et al. [15] proposed a general thin plate theory including surface effects. They derived the governing equations of Kirchhoff and Mindlin plate models including surface effects and provided some numerical examples to verify the validation of the theory. They also concluded that size effects tend to be significant when the thickness of the plate-like thin film structures approach the intrinsic length scale of the materials.

The surrounded elastic medium of SLGS can be assumed as linear (Winkler and Pasternak) or nonlinear elastic medium. Chien et al. [16] investigated nonlinear vibration of laminated plate resting on a nonlinear elastic medium. Using nonlocal elasticity theory of orthotropic plate Ghorbanpour Arani et al. [17] carried out vibration analysis of the coupled system of doubled-layered

graphene sheets (CS-DLGSs) embedded in a Visco-Pasternak foundation. The two DLGSs were coupled by an enclosing viscoelastic medium which is simulated as a Visco-Pasternak foundation. Vibration characteristics of a simple supported viscoelastic nanoplate were studied by Pouresmaeeli et al. [18] using nonlocal plate theory and including the effect of viscoelastic foundation. Their results showed that the frequency significantly decreases with an increase in the damping coefficient of foundation.

Since the mechanical behaviors of nanostructures such as nanotubes and nanoplates become significant in designing many nano-electro-mechanical devices, nanosensors and nanoactuators, a large amount of studies were conducted on the vibration, instability and wave propagation characteristics of such structures. Wang et al. [19] studied the impact of the longitudinal magnetic field on wave propagation in carbon nanotubes embedded in the elastic matrix. The effect of an in-plane magnetic field on the transverse vibration of a magnetically sensitive SLGS using equivalent continuum nonlocal elastic plate theory was examined by Murmu et al. [20]. They showed that the in-plane field increases the natural frequencies of the SLGS. Moreover, nonlocal effects are dampened by the in-plane magnetic field exerted on SLGS.

However, to the best of author's knowledge no report has been found in the literature on the vibration analysis of a viscoelastic SLGS focusing on surface effects. Motivated by these considerations, we aim to study the surface effects on the vibration characteristics of a viscoelastic SLGS embedded on Visco-Pasternak elastic foundation based on nonlocal elasticity theory. Herein the SLGS is subjected to the magnetic field in x-directions. An analytical method is employed to obtain the frequency of the system. An investigation will be made into the effect of small scale parameters, surface layers, aspect ratio of thickness to length, magnetic field, Visco-Pasternak elastic medium and viscoelastic structural damping coefficient of graphene sheet. Moreover, a comparison between the findings of the present study and the results found in the literature show the accuracy of the current research.

2. BASIC EQUATIONS

2.1 Preliminaries

The coordinate system of the middle surface of plate are x, y and z that are taken for the length, width and thickness of the graphene sheet, respectively (See Fig. 1). Consider a SLGS as depicted in Fig. 1 which shows the geometrical parameters of length b, width l and thickness h. The SLGS is rested on an elastic medium which is simulated by Visco-Pasternak foundation and it is also subjected to a magnetic field.

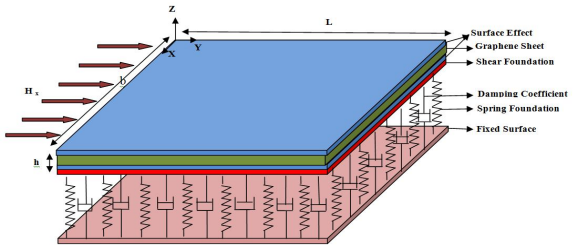

Fig. 1. Schematic of an embedded SLGS embedded on Visco-Pasternak foundation.

As is well known, this foundation model is both capable of transverse shear loads (k_g), normal loads (k_w) and also damping structural coefficient (c). According to classical laminated plate theory (CLPT) which is used in the present formulation, the displacements of any arbitrary point of the graphene sheet along x, y and z directions (u, v and w) can be expressed as [17]:

$$(x,y,z,t) = -z\,\frac{\partial w_0(x,y,t)}{\partial x}, \tag{1a}$$

$$(x,y,z,t) = -z\,\frac{\partial w_0(x,y,t)}{\partial y}, \tag{1b}$$

$$(x,y,z,t) = w_0(x,y,t), \tag{1c}$$

where w_0 is the displacement of the mid surface of the plate along z direction. The Von Karman-type nonlinear strain relations are used here which can be expressed as:

$$\varepsilon_{xx} = \frac{\partial u}{\partial x} + \frac{1}{2}\left(\frac{\partial w}{\partial x}\right)^2 = -z\,\frac{\partial^2 w_0}{\partial x^2} + \frac{1}{2}\left(\frac{\partial w_0}{\partial x}\right)^2, \tag{2a}$$

$$\varepsilon_{yy} = \frac{\partial u}{\partial y} + \frac{1}{2}\left(\frac{\partial w}{\partial y}\right)^2 = -z\,\frac{\partial^2 w_0}{\partial y^2} + \frac{1}{2}\left(\frac{\partial w_0}{\partial y}\right)^2, \tag{2b}$$

$$\begin{aligned}\gamma_{xy} &= \frac{\partial u}{\partial y} + \frac{\partial v}{\partial x} + \frac{\partial w}{\partial x}\frac{\partial w}{\partial y} \\ &= \frac{\partial w_0}{\partial x}\frac{\partial w_0}{\partial y} - 2z\frac{\partial^2 w_0}{\partial x \partial y}.\end{aligned} \tag{2c}$$

2.2. Magnetic field

The governing electrodynamics Maxwell equations for a perfectly conducting elastic body are given by [21]:

$$Curl\,\vec{e} = -\eta\frac{\partial \vec{h}}{\partial t}, \tag{3a}$$

$$\vec{J} = Curl\,\vec{h}, \tag{3b}$$

$$div\,\vec{h} = 0, \tag{3c}$$

$$\vec{e} = -\eta\left(\frac{\partial \vec{U}}{\partial t} \times \vec{H}\right), \tag{3d}$$

$$\vec{h} = Curl\left(\vec{U} \times \vec{H}\right), \tag{3e}$$

where $\vec{J}$ is the electric current density vector, $\vec{e}$ perturbation of electric field vector, $\vec{h}$ perturbation of magnetic field vector, $\vec{U}$ displacement vector and η is the magnetic permeability.

Imposing a magnetic field vector in longitudinal direction $\vec{H} = (H_x, 0, 0)$, assuming $\vec{U} = (u_0, v_0, w_0)$ and using Eqs. (3) yields:

$$\begin{aligned}h = &\left(-\frac{\partial v_0}{\partial y}H_x - \frac{\partial w_0}{\partial z}H_x\right)\hat{i} + \\ &\left(\frac{\partial v_0}{\partial x}H_x\right)\hat{j} + \left(\frac{\partial w_0}{\partial x}H_x\right)\hat{k},\end{aligned} \tag{4}$$

Therefore the Lorentz force can be obtained as:

$$F_e = \eta(J \times H) \Rightarrow F_e = -\eta H_x^2\left(\frac{\partial^2 w_0}{\partial x^2}\right). \tag{5}$$

2.3. Nonlocal elasticity theory

Based on Eringen's nonlocal elasticity, the stress tensor is not only affected from its own reference point but it also receives pressure from all other points of the body. The nonlocal constitutive behavior can be given as follows [20]:

$$\sigma_{ij}^{nl}(x) = \int_v \alpha(|x - x'|, \tau)\sigma_{ij}^{l} dV(x'), \quad \forall x \in V \tag{6}$$

where σ_{ij}^{nl} and σ_{ij}^{l} are, the nonlocal stress tensor and local stress tensors, respectively; $\alpha(|x - x'|, \tau)$ is the nonlocal modulus; $|x - x'|$ is the Euclidean distance, and $\tau = e_0 a / l$ in which l is the external characteristic length, e_0 denotes constant appropriate to each material, and a is an internal characteristic length of the material. Consequently, $e_0 a$ is a constant parameter which is obtained with molecular dynamics, experimental results, experimental studies and molecular structure mechanics. The constitutive equation of the nonlocal elasticity can be written as [19]:

$$(1 - \mu\nabla^2)\sigma^{nl} = \sigma^{l}, \tag{7}$$

where the parameter $\mu = (e_0 a)^2$ denotes the small scale effect on the response of structures in nanosize, and ∇^2 is the Laplacian operator in the above equation and can be expressed as $\nabla^2 = \partial^2/\partial x^2 + \partial^2/\partial y^2$. Also σ^{nl} and σ^{l} are nonlocal and local stresses, respectively.

Employing the energy method and Hamilton's principle yields the following nonlocal linear motion equation for transverse vibration of the SLGS as:

$$\begin{aligned}&\frac{\partial^2 M_{xx}}{\partial x^2}+\frac{\partial^2 M_{yy}}{\partial y^2}+2\frac{\partial^2 M_{xy}}{\partial x\partial y}+\left(1-(e_0a)^2\nabla^2\right)\times\\&\left(\eta H_x^2\left(\frac{\partial^2 w_0}{\partial x^2}\right)-k_w w_0+k_g\frac{\partial^2 w_0}{\partial x^2}-c\frac{\partial w_0}{\partial t}\right)=\\&\left(1-(e_0a)^2\nabla^2\right)m_0\frac{\partial^2 w_0}{\partial t^2}-\left(1-(e_0a)^2\nabla^2\right)\times\\&m_2\left(\frac{\partial^4 w_0}{\partial t^2\partial x^2}+\frac{\partial^4 w_0}{\partial t^2\partial y^2}\right),\end{aligned}\tag{8}$$

in which:

$$\begin{Bmatrix}M_{xx}\\M_{yy}\\M_{xy}\end{Bmatrix}=\int_{-h/2}^{h/2}\begin{Bmatrix}\sigma_{xx}\\\sigma_{yy}\\\sigma_{xy}\end{Bmatrix}zdz\,,\begin{Bmatrix}m_0\\m_2\end{Bmatrix}=\int_{-h/2}^{h/2}\rho\begin{Bmatrix}1\\z^2\end{Bmatrix}dz\,,\tag{9}$$

2.4. Surface effects

In order to study the effect of surface layer in nanostructure mechanical behaviors, Gurtin and Murdoch [22, 23] presented a model in which the surface layer is assumed as a mathematical layer with zero thickness and different material properties. According to this theory, the following equation can be written for surface-strain relation [24]:

$$\begin{aligned}\sigma_{\alpha\beta}^s=&\tau^s\delta_{\alpha\beta}+\left(\tau^s+\lambda^s\right)\varepsilon_{kk}\delta_{\alpha\beta}+\\&2\left(\mu^s-\tau^s\right)\varepsilon_{\alpha\beta}+\tau^s u_{\alpha,\beta}^s,\end{aligned}\tag{10}$$

where λ^s and μ^s are the Lame constants of surface layer; τ^s is the residual stress under unconstrained conditions; $\delta_{\alpha\beta}$ is the Kronecker delta. Using Eq. (10) the following surface equations are given:

$$\begin{aligned}\sigma_x^s=&\tau^s+\left(2\mu^s+\lambda^s\right)\frac{\partial u}{\partial x}+\left(\lambda^s+\tau^s\right)\frac{\partial v}{\partial y}\\&\pm\frac{h}{2}\left(\left(2\mu^s+\lambda^s\right)\frac{\partial^2 w}{\partial x^2}+\left(\lambda^s+\tau^s\right)\frac{\partial^2 w}{\partial y^2}\right),\end{aligned}\tag{11a}$$

$$\begin{aligned}\sigma_y^s=&\tau^s+\left(2\mu^s+\lambda^s\right)\frac{\partial v}{\partial x}+\left(\lambda^s+\tau^s\right)\frac{\partial u}{\partial y}\\&\pm\frac{h}{2}\left(\left(2\mu^s+\lambda^s\right)\frac{\partial^2 w}{\partial y^2}+\left(\lambda^s+\tau^s\right)\frac{\partial^2 w}{\partial x^2}\right),\end{aligned}\tag{11b}$$

$$\sigma_{xy}^s=\pm\left(2\mu^s-\tau^s\right)\frac{\partial^2 w}{\partial y\,\partial x},\tag{11c}$$

$$\sigma_{yz}^s=\tau^s\frac{\partial w}{\partial y},\tag{11d}$$

$$\sigma_{xz}^s=\tau^s\frac{\partial w}{\partial x}.\tag{11e}$$

Using Eqs. (9) and (11) yields the moment resultants of the surface layers $\left\{M_x^s\quad M_y^s\quad M_{xy}^s\right\}$ as:

$$M_x^s=\frac{h^2}{2}\left(\begin{matrix}\left(2\mu^s+\lambda^s\right)\frac{\partial^2 w}{\partial x^2}\\+\left(\lambda^s+\tau^s\right)\frac{\partial^2 w}{\partial y^2}\end{matrix}\right),\tag{12a}$$

$$M_y^s=\frac{h^2}{2}\left(\begin{matrix}\left(2\mu^s+\lambda^s\right)\frac{\partial^2 w}{\partial y^2}\\+\left(\lambda^s+\tau^s\right)\frac{\partial^2 w}{\partial x^2}\end{matrix}\right),\tag{12b}$$

$$M_{xy}^s=\left(2\mu^s-\lambda^s\right)\frac{h^2}{2}.\tag{12c}$$

According to Gurtin-Murdoch model andunlike classical plate theories, σ_{zz} is not equal to zero on the upper and lower surfaces. Indeed, the stress component σ_{zz} varies linearly along the graphene sheet thickness and satisfies the balance condition on the surfaces which can be expressed as the following relation:

$$\sigma_{zz}=\frac{1}{2}\left(\sigma_z^+ +\sigma_z^-\right)+\frac{z}{h}\left(\sigma_z^+ -\sigma_z^-\right)$$
$$=\frac{1}{2}\left(\frac{\partial\sigma_{xz}^s}{\partial x}+\frac{\partial\sigma_{yz}^s}{\partial y}-\rho^s\frac{\partial^2 w}{\partial t^2}\right)^+$$
$$+\frac{1}{2}\left(\frac{\partial\sigma_{xz}^s}{\partial x}+\frac{\partial\sigma_{yz}^s}{\partial y}-\rho^s\frac{\partial^2 w}{\partial t^2}\right)^- +\qquad (13)$$
$$\frac{z}{2}\left(\frac{\partial\sigma_{xz}^s}{\partial x}+\frac{\partial\sigma_{yz}^s}{\partial y}-\rho^s\frac{\partial^2 w}{\partial t^2}\right)^+$$
$$-\frac{z}{2}\left(\frac{\partial\sigma_{xz}^s}{\partial x}+\frac{\partial\sigma_{yz}^s}{\partial y}-\rho^s\frac{\partial^2 w}{\partial t^2}\right).$$

Considering Eq. (13) the following stress component in transverse direction can be obtained as:

$$\sigma_{zz}=\frac{2z}{h}\left(\tau^s\frac{\partial^2 w}{\partial x^2}+\tau^s\frac{\partial^2 w}{\partial y^2}-\rho^s\frac{\partial^2 w}{\partial t^2}\right),\qquad (14)$$

in which ρ^s is the pass density of the surface layer. On the other hand, the local stress strain relation for the bulk material (graphene sheet) can be written as follows:

$$\sigma_{ij}=\lambda\varepsilon_{kk}\delta_{ij}+2\mu\varepsilon_{ij},\qquad (15)$$

where λ and μ are the Lame constants, σ_{ij} and ε_{ij} are the local stress and strain components, in which:

$$\varepsilon_{ij}=\frac{1}{2}\left(u_{i,j}+u_{j,i}\right),\qquad (16)$$

Using Eqs. (14) and (15) yields the stress strain relations for the bulk material as follows:

$$\sigma_{i\beta}=\frac{E}{1+\nu}\left(\varepsilon_{i\beta}+\frac{\nu}{1-\nu}\varepsilon_{\gamma\gamma}\delta_{i\beta}\right)+\frac{\nu}{1-\nu}\sigma_{zz}\delta_{i\beta}\qquad (17)$$

where E and ν are the Young's modulus and Poisson's ratio, respectively.

Substituting Eqs. (17) into Eq. (9) and using Eq. (14) yields the moment resultants of the bulk material $\left\{M_x^b \quad M_y^b \quad M_{xy}^b\right\}$ as:

$$M_x^b=-\frac{Eh^3}{12\left(1-\nu^2\right)}\left(\frac{\partial^2 w}{\partial x^2}+\nu\frac{\partial^2 w}{\partial y^2}\right)+$$
$$\frac{\nu h^2\tau^s}{6(1-\nu)}\left(\frac{\partial^2 w}{\partial x^2}+\frac{\partial^2 w}{\partial y^2}\right)-\frac{\nu h^2\rho^s}{6(1-\nu)}\frac{\partial^2 w}{\partial t^2},\qquad (18a)$$

$$M_y^b=-\frac{Eh^3}{12\left(1-\nu^2\right)}\left(\frac{\partial^2 w}{\partial y^2}+\nu\frac{\partial^2 w}{\partial x^2}\right)+$$
$$\frac{\nu h^2\tau^s}{6(1-\nu)}\left(\frac{\partial^2 w}{\partial x^2}+\frac{\partial^2 w}{\partial y^2}\right)-\frac{\nu h^2\rho^s}{6(1-\nu)}\frac{\partial^2 w}{\partial t^2},\qquad (18b)$$

$$M_{xy}^b=\frac{-Eh^3}{12(1+\nu)}\frac{\partial^2 w}{\partial x\,\partial y}.\qquad (18c)$$

2.5. Viscoelastic property of SLGS

Based on Kelvin's model on elastic materials, the Young's modulus is replaced with $E\left(1+g\,\partial/\partial t\right)$ [19], in which g is the viscoelastic structural damping coefficient.

Substituting Eqs. (12) and (18) into Eq. (8) and using Kelvin's model for viscoelastic property of SLGS yields the following motion equation:

$$\frac{-Eh^3}{12\left(1-\nu^2\right)}\left(\frac{\partial^4 w}{\partial x^4}+2\nu\frac{\partial^4 w}{\partial x^2\partial y^2}+\frac{\partial^4 w}{\partial y^4}\right)-$$
$$\frac{Eh^3 g}{12\left(1-\nu^2\right)}\left(\frac{\partial^5 w}{\partial x^4\partial t}+2\nu\frac{\partial^5 w}{\partial x^2\partial y^2\partial t}+\frac{\partial^5 w}{\partial y^4\partial t}\right)+$$
$$\frac{h^2}{2}\left(2\mu^s+\lambda^s\right)\left(\frac{\partial^4 w}{\partial x^4}+\frac{\partial^4 w}{\partial y^4}\right)+h^2\left(\tau^s+\lambda^s\right)\frac{\partial^4 w}{\partial x^2\partial y^2}+$$
$$\frac{\nu h^2\tau^s}{6(1-\nu)}\left(\frac{\partial^4 w}{\partial x^4}+2\frac{\partial^4 w}{\partial x^2\partial y^2}+\frac{\partial^4 w}{\partial y^4}\right)-\frac{Eh^3}{6(1+\nu)}\frac{\partial^4 w}{\partial x^2\partial y^2}-$$
$$\frac{Eh^3 g}{6(1+\nu)}\frac{\partial^5 w}{\partial x^2\partial y^2\partial t}+2\tau^s\left(1-(e_0a)^2\nabla^2\right)\left(\frac{\partial^4 w}{\partial x^4}+\frac{\partial^4 w}{\partial y^4}\right)+\qquad (19)$$
$$\left(1-(e_0a)^2\nabla^2\right)q+\frac{\partial}{\partial x}\left(1-(e_0a)^2\nabla^2\right)\left(N_x\frac{\partial w}{\partial x}\right)+$$
$$\frac{\partial}{\partial y}\left(\left(1-(e_0a)^2\nabla^2\right)N_y\frac{\partial w}{\partial y}\right)=$$
$$\left(1-(e_0a)^2\nabla^2\right)\left(m_0+2\rho^s\right)\frac{\partial^2 w}{\partial t^2}-$$

$$\left(1-\left(e_0 a\right)^2 \nabla^2\right) m_2 \left(\frac{\partial^4 w}{\partial t^2 \partial x^2}+\frac{\partial^4 w}{\partial t^2 \partial y^2}\right),+$$
$$\frac{\rho^s \nu h^2}{6(1-\nu)}\left(\frac{\partial^4 w}{\partial t^2 \partial x^2}+\frac{\partial^4 w}{\partial t^2 \partial y^2}\right).$$

3. SOLUTION METHOD

In this section, an analytical method is used to solve the motion equation. For this purpose, the Navier method for simply supported graphene sheet can be used as follows:

$$w=\sum_{m=1}^{\infty}\sum_{n=1}^{\infty}\sin\left(\frac{m\pi}{b}x\right)\left(\frac{n\pi}{l}y\right)e^{i\omega t}, \tag{20}$$

where A_{mn} is the amplitude, ω is the (Fundamental) natural frequency, and m and n are half wave numbers.

Defining dimensionless parameters as:

$$\overline{w}=\frac{w}{h},\beta=\frac{h}{l},\Gamma=\frac{y}{l},\varsigma=\frac{x}{b},s=\frac{b}{l},$$
$$K_w=\frac{k_w h}{E},K_g=\frac{k_g}{El},e_n=\frac{e_0 a}{l},\overline{\rho}=\frac{\rho_s}{\rho l},$$
$$\overline{\tau^s}=\frac{\tau^s}{El},\overline{\lambda^s}=\frac{\lambda^s h}{El},\overline{\mu^s}=\frac{\mu^s h}{El},\omega=\frac{\Omega}{l}\sqrt{\frac{E}{\rho}}, \tag{21}$$
$$\bar{t}=\frac{t}{l}\sqrt{\frac{E}{\rho}},G=g\beta\sqrt{\frac{E}{\rho l^2}},C=\frac{c}{\beta^2\sqrt{\rho E}},$$
$$MF=\frac{\eta H_x^2}{E}.$$

Placing Eq. (20) in Eq. (19) and using Eqs. (21), the dimensionless motion equation for transverse vibration of an embedded viscoelastic SLGS subjected to a longitudinal magnetic field can be obtained as:

$$\frac{-1}{12(1-\nu^2)}\left(\beta^4\lambda_n^4+\frac{2\nu\beta^4}{s^2}\lambda_m^2\lambda_n^2+\frac{\beta^4}{s^4}\lambda_m^4\right)-$$
$$\frac{G\Omega\beta^3 i}{12(1-\nu^2)}\left(\lambda_n^4+\frac{2\nu}{s^2}\lambda_m^2\lambda_n^2+\frac{1}{s^4}\lambda_m^4\right)+$$
$$\left(\overline{\mu^s}+\frac{\overline{\lambda^s}}{2}\right)\left(\beta^3\lambda_n^4+\frac{\beta^3}{s^4}\lambda_m^4\right)+\left(\overline{\tau^s}+\overline{\lambda^s}\right)\frac{\beta^3}{s^2}\lambda_m^2\lambda_n^2+$$
$$\frac{\nu\overline{\tau^s}}{6(1-\nu)}\left(\frac{\beta^3}{s^4}\lambda_m^4+2\frac{\beta^3}{s^2}\lambda_m^2\lambda_n^2+\beta^3\lambda_n^4\right)-$$
$$\frac{\beta^4}{6(1+\nu)s^2}\lambda_m^2\lambda_n^2-\frac{G\beta^3\Omega i}{6(1+\nu)}\frac{\lambda_m^2\lambda_n^2}{s^2}-$$
$$2\overline{\tau^s}\left(\frac{\beta}{s^2}\lambda_m^2+\beta\lambda_n^2\right)-2\overline{\tau^s}e_n^2\beta\left(\frac{1}{s^4}\lambda_m^4+\frac{2}{s^2}\lambda_m^2\lambda_n^2+\lambda_n^4\right)+$$
$$-\overline{N_x}\beta\lambda_n^2-\overline{N_y}\frac{\beta}{s^2}\lambda_m^2-e_n^2\overline{N_x}\frac{\beta}{s^2}\lambda_m^2\lambda_n^2-e_n^2\overline{N_y}\frac{\beta}{s^4}\lambda_m^4-$$
$$e_n^2\overline{N_y}\frac{\beta}{s^2}\lambda_m^2\lambda_n^2-K_w-K_w e_n^2\left(\lambda_n^2+\frac{\lambda_m^2}{s^2}\right)+K_g\beta\left(\lambda_n^2+\frac{\lambda_m^2}{s^2}\right)+ \tag{22}$$
$$iK_g G\Omega\left(\lambda_n^2+\frac{\lambda_m^2}{s^2}\right)-e_n^2K_g\beta\left(\frac{1}{s^4}\lambda_m^4+\frac{2}{s^2}\lambda_m^2\lambda_n^2+\lambda_n^4\right)$$
$$-ie_n^2K_g G\Omega\left(\frac{1}{s^4}\lambda_m^4+\frac{2}{s^2}\lambda_m^2\lambda_n^2+\lambda_n^4\right)-iC\Omega-$$
$$ie_n^2C\Omega\left(\lambda_n^2+\frac{\lambda_m^2}{s^2}\right)-MF\beta^2\left(\lambda_n^2+\frac{\lambda_m^2}{s^2}\right)-$$
$$e_n^2MF\beta^2\left(\frac{1}{s^4}\lambda_m^4+\frac{2}{s^2}\lambda_m^2\lambda_n^2+\lambda_n^4\right)=$$
$$-\left(\beta^2+2\overline{\rho}\beta\right)\Omega^2-e_n^2\Omega^2\left(\frac{\beta^2}{s^4}\lambda_m^2+\beta^2\lambda_n^2+2\overline{\rho}\beta\lambda_n^2+\frac{2\overline{\rho}\beta\lambda_m^2}{s^2}\right)-$$
$$\frac{\Omega^2\beta^4}{12}\left(\frac{1}{s^2}\lambda_m^2+\lambda_n^2\right),-$$
$$\frac{e_n^2\beta^4\Omega^2}{12}\left(\frac{1}{s^4}\lambda_m^4+\frac{2}{s^2}\lambda_m^2\lambda_n^2+\lambda_n^4\right)+\frac{\overline{\rho}\nu\Omega^2\beta^3}{6(1-\nu)}\left(\frac{1}{s^2}\lambda_m^2+\lambda_n^2\right),$$

in which $\lambda_m=m\pi$ and $\lambda_n=n\pi$. The real part of frequency corresponds to the system damping, and the imaginary part represents the system natural frequencies.

4. NUMERICAL RESULTS AND DESCUSSION

The following section discusses in detail the effect of surface layers, nonlocal parameter, length of graphene sheet, elastic medium, mode numbers, magnetic field and aspect ratio of the SLGS

The mechanical and electrical characteristics of a SLGS, the surrounding elastic medium and the nonlocal parameters have been employed [16, 17].

Fig. 2 depicts the dimensionless natural frequency versus dimensionless small scale parameter for different values of damper modulus parameter of the elastic medium. It is seen that the dimensionless

natural frequency of SLGS decreases as the damper modulus parameter of the elastic medium increases. Also it can be observed that the dimensionless natural frequency is decreased with an increase in the small scale parameter until it reaches the zero value where instability occurs in the system. Therefore, it can be concluded that the system loses its stability at higher small scale parameter values. This is because increasing the nonlocal parameter implies decreasing interaction force between graphene sheet atoms, and that leads to a softer structure. Furthermore, the small scale effects on the dimensionless natural frequency become more distinguished at higher damper modulus of elastic medium values.

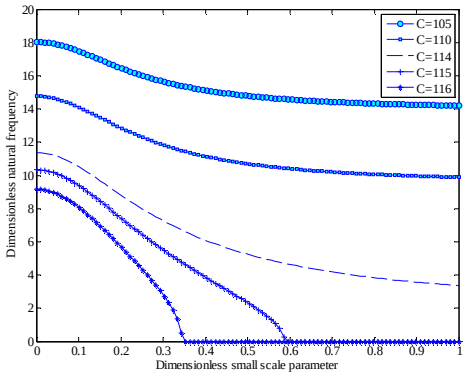

Fig. 2. Effect of damper modulus parameter of the elastic medium on the dimensionless natural frequency with respect to the dimensionless small scale parameter.

The effects of the magnetic field on the dimensionless natural frequency with respect to the aspect ratio of thickness to length are illustrated in Fig. 3 with $C = 114$ and $e_n = 1$. As can be seen, the dimensionless natural frequency decreases as the aspect ratio increases since the system becomes unstable at zero dimensionless natural frequency value. It is also seen that the magnetic field plays an important role in vibration characteristics of SLGS. Enhancing the magnetic field increases the natural frequency. Hence, it is possible to improve the stability of the system by enhancing the magnetic field.

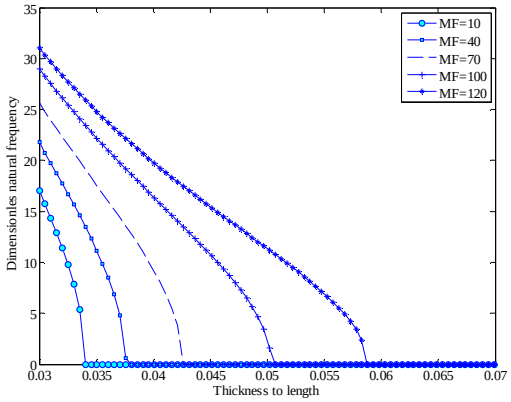

Fig. 3. Effect of the magnetic field on the dimensionless natural frequency with respect to the aspect ratio.

Fig. 4 demonstrates the effect of the surface density on the dimensionless natural frequency with respect to the aspect ratio of the thickness to length. It can be found that the natural frequency of the system increases at a decreasing rate with an increase in the density of surface layers. Also the variations of dimensionless natural frequency become more prominent at lower surface density values. It is worth mentioning that an increase in the thickness to length ratio of the SLGS leads to lower natural frequencies. In other words, the SLGS is more stable at lower thickness to length ratio values.

The variation of dimensionless natural frequency versus dimensionless small scale parameter for different viscoelastic structural damping coefficients is depicted in Fig. 5 with $C = 10$, $MF = 10$, $K_w = 286$ and $K_g = 2.86$.

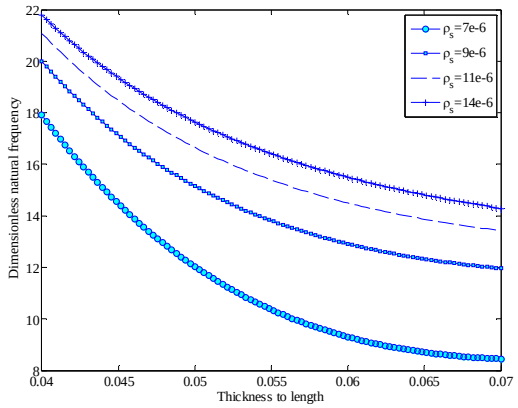

Fig. 4. Effect of the surface density on the dimensionless natural frequency with respect to the aspect ratio.

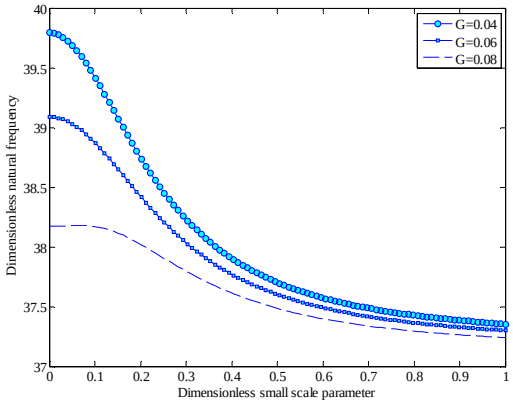

Fig. 5. Dimensionless natural frequency versus dimensionless small scale parameter for different viscoelastic structural damping coefficients.

It can be found that increasing the viscoelastic structural damping coefficient of SLGS lowers the dimensionless natural frequency. This is because increasing the structural damping coefficient yields looser structure. It is also seen that the effect of viscoelastic structural damping coefficient becomes more visible at lower small scale parameters.

To realize the effect of the Winkler and Pasternak coefficients of elastic medium, Fig. 6 shows how dimensionless natural frequency changes with respect to the dimensionless Winkler modulus for different values of Pasternak coefficient with $C=10$, $MF=10$, $e_n=1$. The findings indicate that an increase in the dimensionless Winkler (K_w) and Pasternak (K_g) coefficients increases the dimensionless natural frequency of the system. It is due to the fact that increasing K_w and K_g increases the structure stiffness and hence the stability of SLGS.

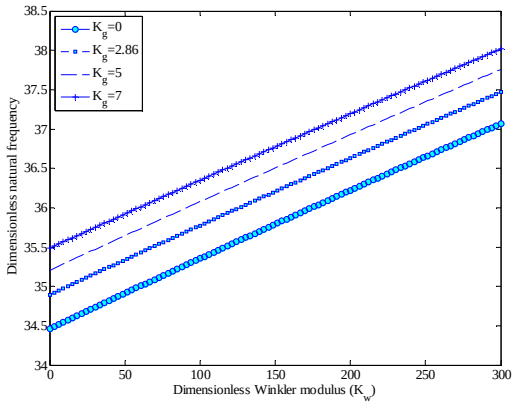

Fig. 6. Effects of Winkler and Pasternak coefficients on the dimensionless natural frequency.

5. Conclusion

In this study, transverse vibration characteristics of a SLGS are examined using nonlocal elasticity theory. The graphene sheet is subjected to a longitudinal magnetic field and also embedded on a Visco-Pasternak elastic medium. By considering surface effects, the motion equation of SLGS is derived. An analytical method is employed to obtain the damping and natural frequencies so that the effects of small scale parameter, elastic medium, aspect ratio of thickness to length, magnetic field, surface layers and viscoelastic structural damping coefficient are studied in detail. The following conclusions may be made from the findings:

The natural frequency of SLGS decreases as the small scale parameter increases. Frequency

decreases the viscoelastic structural damping coefficient and damper modulus parameter of elastic medium increases. The stiffness and hence the frequency of the SLGS increases with an increase in Winkler and Pasternak coefficients. Natural frequency and stability of the system increases as the magnetic field and density of surface layers increase.

Acknowledgments

The authors would like to thank the referees for their valuable comments. The authors are grateful to University of Kashan for supporting this work by Grant no. 65475/71. They would also like to thank the Iranian Nanotechnology Development Committee for their financial support.

References

[1] A. Sakhaee-Pour, Solid State Commun. 149 (2009) 91.

[2] C. Chen, W. Fu, C. Yu, Mater. Lett. 82 (2012) 33.

[3] C. Baykasoglu, A. Mugan, Comput. Mater. Sci. 55(2012) 228.

[4] Y. Qian, C. Wang, Z.G .Le, Appl. Surf. Sci., 257(2011)10758.

[5] A. Sakhaee-Pour, M.T. Ahmadian., A. Vafai, Solid State Commun. 145 (2008)168.

[6] R. Ansari, S. Sahmani, B. Arash, Phys. Lett. A 375 (2010) 53.

[7] R.C. Pradhan, A. Kumar, Comput. Mater. Sci. 50 (2010) 239.

[8] A.C. Eringen, J. Appl. Phys. 54 (1983) 4703.

[9] S.C. Pradhan, T. Murmu, Physica E 42(2010)1293.

[10] T. Murmu, S.C. Pradhan, Physica E, 41(2009)1628.

[11] L.Shena, H.S. Shena, C.L Zhang, Comput. Mater. Sci. 48(2010) 680.

[12] M.S. Ciu, T. Chen, Eng. Proced, 10 (2011) 297.

[13] A. Assadi, Appl. Math. Model. 37 (2013) 3575.

[14] S.P.A. Gill, Int. J. Solids and Struct. 44 (2007) 7500.

[15] P. Lu, L.H. He, H.P. Lee, C. Lu, 43 (2006) 4631.

[16] R.D. Chien, C.S. Chen, Compos. Struct. 70 (2005), 90.

[17] A. Ghorbanpour Arani, A. Shiravand, M. Rahi, R. Kolahchi, Physica B, 407(2012) 4123.

[18] S. Pouresmaeeli, E. Ghavanloo, S.A. Fazelzadeh, Compos. Struct. 96 (2013) 405.

[19] H. Wang, K. Dong, F. Men, Y. Yan, X. Wang, Appl. Math. Model. 34(2010) 878.

[20] T. Murmu, M.A. McCarthy, S. Adhikari, Compos. Struct. 96(2013) 57.

[21] A. Loghman, M. Abdollahian, A. Jafarzadeh Jazi, A. Ghorbanpour Arani, Int. J. Therm. Sci., 65(2013) 254.

[22] M.E. Gurtin, A.I. Murdoch, Arch. of Rot. Mech. and Anal. 57(1975) 291.

[23] M.E. Gurtin, A.I. Murdoch, Int. J. of solids Struct. 14 (1978) 431.

[24] A. Ansari, S. Sahmani, Int. J. Eng. Sci. 49(2011) 1204.